

See discussions, stats, and author profiles for this publication at: <https://www.researchgate.net/publication/51903585>

# Strain Tunes Proteolytic Degradation and Diffusive Transport in Fibrin Networks

ARTICLE in BIOMACROMOLECULES · DECEMBER 2011

Impact Factor: 5.75 · DOI: 10.1021/bm2015619 · Source: PubMed

CITATIONS

3

READS

6

## 3 AUTHORS:



**Arjun Adhikari**

Stanford Medicine

**14** PUBLICATIONS **104** CITATIONS

SEE PROFILE



**Armen Mekhdjian**

Stanford University

**7** PUBLICATIONS **70** CITATIONS

SEE PROFILE



**Alexander R Dunn**

Stanford University

**58** PUBLICATIONS **1,075** CITATIONS

SEE PROFILE

Published in final edited form as:

*Biomacromolecules*. 2012 February 13; 13(2): 499–506. doi:10.1021/bm2015619.

## Strain tunes proteolytic degradation and diffusive transport in fibrin networks

Arjun S. Adhikari, Armen H. Mekhdjian, and Alexander R. Dunn\*

Department of Chemical Engineering, Stanford University, Stanford, CA 94305

### Abstract

Proteolytic degradation of fibrin, the major structural component in blood clots, is critical both during normal wound healing and in the treatment of ischemic stroke and myocardial infarction. Fibrin-containing clots experience substantial strain due to platelet contraction, fluid shear, and mechanical stress at the wound site. However, little is understood about how mechanical forces may influence fibrin dissolution. We used video microscopy to image strained fibrin clots as they were degraded by plasmin, a major fibrinolytic enzyme. Applied strain causes up to 10-fold reduction in the rate of fibrin degradation. Analysis of our data supports a quantitative model in which the decrease in fibrin proteolysis rates with strain stems from slower transport of plasmin into the clot. We performed fluorescence recovery after photobleaching (FRAP) measurements to further probe the effect of strain on diffusive transport. We find that diffusivity perpendicular to the strain axis decreases exponentially with increasing strain, while diffusivity along the strain axis remains unchanged. Our results suggest that the properties of the fibrin network have evolved to protect mechanically loaded fibrin from degradation, consistent with its function in wound healing. The pronounced effect of strain upon diffusivity and proteolytic susceptibility within fibrin networks offers a potentially useful means of guiding cell growth and morphology in fibrin-based biomaterials.

### Introduction

The formation and dissolution of fibrin networks, a major structural component of blood clots, is a critical physiological process. Careful regulation is necessary to avoid thrombosis on the one hand, and uncontrolled bleeding on the other<sup>1–5</sup>. Fibrin is also utilized as a tissue engineering scaffold<sup>6–8</sup> and as a glue in wound healing applications<sup>9,10</sup>. Both physiological and engineered fibrin networks are subject to strain resulting from mechanical stress at a wound or implantation site. Blood clots are likewise subject to deformation under the action of platelet contraction<sup>11</sup> and blood flow<sup>12</sup>. Fibrin networks can extend to over twice their resting length under strain thus making fibrin well suited to bear mechanical load<sup>13–15</sup>.

Understanding the physical parameters that modulate fibrin network degradation is thus of considerable medical importance. Recently, it has been shown that mechanical strain slows down fibrin proteolytic degradation through an unknown mechanism<sup>16,17</sup>. Stretching most materials, for instance a copper wire, leads to increased length, increased surface area, and hence an increased surface-to-volume ratio. Since the proteolytic degradation of fibrin occurs at the clot surface, increased strain might therefore be expected to lead to more

Corresponding Author: Alexander Dunn, Dept. of Chemical Engineering, Stanford University, 381 North-South Mall, Stanford, CA 94035. tel: 650-714-7158, alex.dunn@stanford.edu.

Supporting information

A detailed description of data analysis, alternative model and supporting figures is provided in the supporting information. This material is available free of charge via the Internet at <http://pubs.acs.org>.

surface area and hence *faster* degradation, not slower as is observed. Slower fibrin degradation under load is, in principle, beneficial in the context of wound healing. Conversely, hindered proteolysis is antithetical to rapid clot dissolution during the treatment of a thrombus-induced heart attack or stroke.

Here we examine the mechanism by which mechanical strain protects fibrin from proteolytic degradation. In line with previously reported data, we find that mechanical strain increases fibril alignment<sup>13,18</sup>, decreases clot volume<sup>13</sup>, and decreases enzymatic degradation<sup>16</sup>. Further, we observe that strain markedly decreases the rate of macromolecular diffusion perpendicular to, but not along, the axis of applied load. Control experiments indicate that the decrease in proteolysis observed in strained fibrin networks is not likely to be to the result of irreversible fibrin unfolding. Quantitative analysis of our data supports a model in which the decrease in fibrin proteolysis rates with strain stems from slower transport of plasmin into the clot. The physical properties of fibrin that lead to this result are likely shared by other biomaterials, suggesting that our conceptual framework may be broadly applicable. The marked influence of strain on diffusivity within fibrin networks offers a novel means of controlling molecular concentration gradients, and hence cell growth and differentiation, in fibrin-based biomaterials.

## Materials and Methods

### Materials

Fibrinogen (from human plasma), plasmin (from human plasma), bovine serum albumin (BSA), thrombin, fluorescein isothiocyanate-dextran, D-Val-Leu-Lys-*p*-nitroanilide dichloride (VALY), lysine and TMR-succinimide were purchased from Sigma Aldrich (St. Louis, MO). Factor XIII was purchased from Hematologic Inc. (Essex Junction, VT), perfusion chambers were purchased from Grace Biolabs (Bend, OR), glass capillary tubing was purchased from Wale Apparatus (Hellertown, PA), and PVC tubing was purchased from VWR International (West Chester, PA).

### Crosslinking of fibrinogen to form fibrin gels

Fibrinogen was dissolved to a concentration of 50 mg ml<sup>-1</sup> in sterile water. The lyophilized fibrinogen contained sodium citrate and sodium chloride and the measured pH of the final solution was pH 7.0. Fibrin gels were made using 50 mg ml<sup>-1</sup> fibrinogen, 0.66 IU ml<sup>-1</sup> thrombin, and 5.5 U ml<sup>-1</sup> of Factor XIII. This solution was added to either PVC tubes with an inner diameter (I.D.) of 0.794 mm, or square glass capillary tubing (I.D. 0.7 mm, length 5 cm). Prior to use, the capillary tubes were cleaned by submerging in 12 N HCl for one hour, and then rinsing with copious amounts of milliQ water. The clots were allowed to form at room temperature for 4–5 hours and then stored overnight at 4°C. Immediately before use, the clots were gently pushed out of the capillary by using a thin syringe needle. The clot did not swell or shrink after being taken out of the capillaries. The section of the clot that was in contact with syringe needle was cut off and discarded. Once the clot was out of the tubing, it was kept submerged in buffer (10 mM MES, 100 mM NaCl, pH 7.4) at all times to prevent it from drying.

### Strain assay

Reaction chambers were assembled by attaching perfusion chambers (grace biolabs) (3 × 32 × 0.9 mm) to 3 × 1 inch glass slides. Prior to attaching the perfusion chambers the glass slides were cleaned as described in *Adhikari et al.*<sup>19</sup> To strain the clots, a specified length of the clot was cut (1.6 cm – 4.5 cm) and measured. The clot was strained using tweezers and glued down to the ends of the perfusion chamber using ethyl cyanoacrylate (instant Krazy Glue). The clot was held steady for 10 seconds until it was firmly glued in place. All the

time, the chamber was filled with 10 mM MES, 100 mM NaCl, pH 7.4 to keep the clot hydrated. The chamber was then closed with the chamber coverslip, and the clot was washed with buffer (10 mM MES, 100 mM NaCl, pH 7.4).

### Fibrin proteolysis experiments

Once the fibrin clot was assembled in the reaction chamber,  $1.11 \text{ U mL}^{-1}$  plasmin (10 mM MES, 100 mM NaCl, pH 7.4) was added to the chamber and the fibrin degradation was monitored over time using an upright microscope with 4x objective outfitted with a CMOS camera (Thorlabs) and 4x objective. Data were recorded at 1.02 frames per second.

### Pre-strain assay

Fibrin clots were held at 100% strain for 30–60 seconds, and then allowed to recover for 1 hour. The clot was then mounted in a flow cell, plasmin was introduced in the reaction chamber, and clot ingression over time was monitored as described above.

### Dextran diffusion into strained clots

The diffusion of fluorescently labeled dextran within strained fibrin was analyzed in order to characterize the effect of strain on diffusive transport within the clot. A stock of  $50 \text{ mg mL}^{-1}$  FITC-dextran (70 kD, approximately same molecular weight as plasmin) was first made in sterile water. Clots with a square,  $700 \mu\text{m} \times 700 \mu\text{m}$  in cross section were strained and assembled in the reaction chamber.  $1.25 \text{ mg mL}^{-1}$  FITC-dextran (in 10 mM MES, 100 mM NaCl, pH 7.4) was introduced into the reaction chamber. *z* stacks were taken in the confocal microscope over a period of one hour. The diffusion was monitored at a height of  $\sim 100 \mu\text{m}$  from the bottom of the clot to avoid edge effects due to diffusion from the bottom surface. The diffusivity was analyzed for 10 minutes over the course of the diffusion. Later time points (after 10 minutes) were not analyzed because the effect of diffusion in *z* becomes more apparent at longer times.

### FRAP measurements

FRAP measurements were performed on a Leica TCS SPE confocal microscope. A square region of interest (approximately  $150 \mu\text{m}$  on a side) was selected and photobleached using the maximum possible laser intensity at 488 nm for 60 seconds using a 10x air objective (0.25 N.A. Leica). The low N.A. of the objective ensures that bleaching profile varies slowly in  $z^{20}$ . This allows dextran transport to be approximated as 2D diffusion. Following photobleaching, we imaged FITC-dextran diffusion at much lower laser power. These measurements were repeated at different strains.

## Results

### Mechanical strain increases fibril alignment, decreases clot volume, and decreases enzymatic proteolysis rates

In this study we examine the minimal system of fibrin degradation by activated plasmin. Fibrinolysis *in vivo* is controlled by a complex network of activators, inhibitors and proteases<sup>2</sup>. In our study, the choice of an experimental system comprised of only activated plasmin and fibrin allows us to isolate the effect of mechanical strain on fibrin proteolysis independent of other enzymological complexities.

To study the effect of strain on fibrinolysis, fibrin clots were held at a constant strain in a microfluidic device (Figure 1). Plasmin was added to the microfluidic device, and the proteolysis of the clot was monitored by acquiring a time-lapse movie of the clot

degradation using brightfield illumination. Fluorescent confocal imaging was additionally used to quantify fibril alignment in the strained clots.

Application of strain leads to fibril alignment and an increase in fibrin density, as observed in previous studies<sup>13</sup> (Figure 2). We measured plasmin-mediated degradation of fibrin clots as a function of strain (Figure 2) and observe a steady decrease in clot radius with time (Figure 3a). Fluorescence confocal imaging on FITC-labeled fibrin clots shows that the clots are of uniform density as a function of radius, and that density does not noticeably change during the proteolysis experiment. In all cases, the diameter of the clot as a function of time was well-described by a second order polynomial:

$$d=at^2+v_r t+d_0 \quad \text{eqn 1}$$

Here  $d$  is the diameter of the clot,  $t$  is time,  $d_0$  is the starting diameter, and  $v_r$  is the radial ingression rate. Both  $v_r$  and the rate of total mass removal show marked, ~10 fold decreases with strain (Figure 3b, c). In contrast,  $a$  is close to zero and remains constant across various strains (Figure S1). We tentatively ascribe  $a$  to a gradual, plasmin-independent structural relaxation of the strained clot. Importantly,  $v_r$  scales approximately linearly with fibrin density (Figure 3d). We believe this later observation is significant in understanding how strain affects proteolysis rates (see below).

Decreased fibrinolysis with strain is not likely to stem from a finite amount of plasmin in the flow cell. Proteolysis occurs in a 15–40  $\mu\text{m}$ -wide boundary at the edge of the clot, which is <1% of the total volume of the flow cell. We observe only a 3- to 5-fold enrichment of TMR-labeled plasmin within this boundary layer, indicating that the supply of plasmin is not likely to be rate limiting.

### Diffusion within strained fibrin networks is anisotropic

Fibrin fibrils align under applied load (Figure 2)<sup>13</sup>. Several studies show that solutes diffuse anisotropically in aligned, collagenous biological tissue<sup>21–23</sup>. These observations led us to hypothesize that fibrillar alignment in fibrin might likewise lead to changes in diffusivity.

We monitored the diffusivity of dextrans labeled with fluorescein isothiocyanate (FITC-dextran) in clots strained between 0% and 125% using fluorescence recovery after photobleaching (FRAP)<sup>24</sup>. A section of the clot was photobleached, and the recovery of the bleached area was monitored as a function of time (Figure 4a, b). The kinetics of the recovery of fluorescence in the target region can be modeled according to Fickian diffusion:

$$\frac{\partial C(x, t)}{\partial t} = D \frac{\partial^2 C(x, t)}{\partial x^2} \quad \text{eqn 2}$$

where  $C$  is the concentration of dextran,  $x$  is the direction of diffusion, and  $t$  is time. To accurately determine the diffusivity values from FRAP experiments we implemented a numerical approach using COMSOL Multiphysics finite element simulations in conjugation with MATLAB<sup>25</sup>. Briefly, the first image collected after photobleaching is used as the initial state for the COMSOL finite elements simulation. The evolution of the FITC-dextran distribution is then simulated, assuming different diffusion coefficients parallel and perpendicular to the axis of applied strain. The anisotropic diffusion coefficients are then optimized by comparing the simulation to the experimental FRAP data (Figure 4, Figures S2–5).

Diffusion is isotropic in unstrained clots. As strain increases and the fibrils align in the direction of strain, diffusivity perpendicular to the strain axis (termed radial diffusivity because of the geometry of our system) decreased, while diffusivity along the direction of strain (termed axial diffusivity) remained unaffected (Figure 4, Figure S6). Radial diffusivity decreases exponentially with strain:

$$D_{obs}=D_0\exp(-bs) \quad \text{eq 3}$$

Where  $D_{obs}$  is the radial diffusivity,  $D_0$  is the diffusivity of dextran in absence of strain,  $s$  is the strain, and  $b$  is the exponential decay constant. Although a single exponential fits the data well, it is at present a phenomenological description.

To confirm the FRAP results, we additionally measured the diffusion of FITC-labeled dextran from the bulk solution into the fibrin clots under various strains (Figure S7). The concentration profile at a given  $z$  slice ( $\sim 100 \mu\text{m}$  deep into the clot) was monitored over time, and fit to an analytical 1-D diffusion model<sup>26</sup>. We find that radial diffusivity measured in this fashion decreases with strain, in good agreement with the FRAP experiments.

### **Altered proteolytic susceptibility of fibrin upon force-induced unfolding is not necessary to explain decreased fibrinolysis with strain**

The remarkable ability of fibrin networks to stretch to over twice their resting length is due in large part to the unfolding of fibrin monomers under load<sup>14</sup>. Current data indicate that mechanically-induced unfolding is irreversible<sup>14</sup>. In order to examine the possible effect of strain-induced fibrin unfolding on proteolysis rates, we performed proteolysis measurements on a clot that was first strained, and then allowed to relax for 1 hour. (During this period the clot expands slightly, consistent with the 2<sup>nd</sup>-order term we observe when fitting the proteolysis data for strained clots.) After the clot was allowed to relax, plasmin was introduced to the flow cell, and the proteolytic degradation was monitored as before. The relaxed clots show similar proteolysis dynamics to unstrained clots (Figure 5). Diffusivity within the relaxed clots is isotropic and matched the corresponding unstrained clots to within 20%. The density of the relaxed clots likewise increases by only  $\sim 20\%$  relative to the unstrained clots.

Plasmin accumulates in a narrow,  $< 40 \mu\text{m}$  thick boundary layer at the edge of the clot during proteolysis. We quantified plasmin accumulation in the boundary layer of stretched clots to determine if the plasmin recruitment changes upon strain (Supporting Information). We find that the plasmin accumulation in the boundary layer does not vary appreciably with strain (Figure S11). These data lead us to infer that the plasmin dissociation constant for fibrin also does not change markedly with strain.

In summary, the data discussed above lead us to conclude that the proteolytic susceptibility and plasmin affinity of stretch-unfolded fibrin are similar to native fibrin.

### **An analytical model accounts for changes in proteolysis rates with strain**

Several studies report that strain decreases the rate of proteolytic degradation in multiple biomaterials<sup>16,22,27–30</sup>. However, to our knowledge there is a lack of a unifying model that could account for these observations. In a typical material, volume and density are conserved during deformation. In the case of a cylinder, this leads to an increase in surface area with strain:

$$\frac{S}{S_0} = (1+s)^{1/2} \quad \text{eq 4}$$

Here  $S$  is the surface area,  $S_0$  is surface area before strain is applied, and  $s$  is strain. If fibrin exhibited this behavior,  $v$  should not depend on strain, since density remains unaltered, and the rate of mass removal should increase, since the available surface area increases with strain. Instead, both  $v$  and the rate of mass removal decrease with strain (Figure 3).

We observe that fibrin maintains approximately *constant surface area*, not constant volume, as strain is applied (Figure S8). Consistent with previous work<sup>13</sup>, we hypothesize that this observation stems from the fact that fibrin forms a covalently crosslinked hydrogel. The energetic penalty for breaking covalent crosslinks is therefore anticipated to be higher than the cost of bending and stretching fibrin molecules. The topology of the network is thus preserved under deformation, leading to approximately constant surface area under strain. Volume must therefore decrease as the cylindrical clot is stretched, as we and others observe<sup>13,15</sup>.

These considerations led us to formulate a theoretical treatment that focuses on the relation between fibrin density and degradation rate. The degradation of fibrin can be modeled as an erosion process that takes place in a small boundary layer  $\delta$  at the surface of the clot. We approximate  $\delta$  by equating the timescales for plasmin diffusion and the ingress rate  $v_r$ :

$$t_D \sim \frac{\delta^2}{2D_{eff}}; t_v \sim \frac{\delta}{v_r} \quad \Rightarrow \delta \sim 2 \frac{D_{eff}}{v_r} \quad \text{eq 5}$$

Here  $t_D$  and  $t_v$  are the timescales for diffusion and radial ingress, and  $D_{eff}$  is the effective diffusion constant for plasmin inside the clot. We assume that the rate of fibrin removal is proportional to the local plasmin concentration at a given radial coordinate:

$$\left. \frac{dF}{dt} \right|_r = -kP \quad \text{eq 6}$$

Assuming  $r \gg \delta$ , the rate of fibrin removal (moles  $s^{-1}$ ) is:

$$\frac{d\Phi}{dt} = -k\langle P \rangle 2\pi r \delta L \quad \text{eq 7}$$

where  $\Phi$  is moles fibrin,  $\langle P \rangle$  is the average plasmin concentration within the boundary layer, and  $L$  is the clot length. The change in  $\Phi$  along the radial axis is:

$$\frac{d\Phi}{dr} = F \cdot 2\pi r L \quad \text{eq 8}$$

The change in clot radius with time is therefore:

$$\frac{dr}{dt} = \frac{d\Phi/dt}{d\Phi/dr} = \frac{-k\langle P \rangle}{F} \delta \quad \text{eq 9}$$

The rate of clot radius decrease  $v_r$  is



$$v_r = -\frac{dr}{dt} = k \frac{\langle P \rangle}{F} \delta \quad \text{eq 10}$$

The effective diffusion constant  $D_{eff}$  scales approximately linearly with the plasmin dissociation constant ( $K_D$ ) for fibrin:

$$D_{eff} = D \frac{K_D}{F} \quad \text{eq 11}$$

Here  $D$  is the radial plasmin diffusion constant in the absence of fibrin binding. Combining equations 5, 10 and 11 yields:

$$v_r \sim \frac{1}{F} (2k\langle P \rangle D k_D)^{\frac{1}{2}} \quad \text{eq 12}$$

Eqn. 12 correctly predicts that  $v_r$  scales approximately inversely with  $F$  (Figure 3d).  $v_r$  also depends on  $D^{1/2}$ , suggesting that decreased radial diffusivity also contributes to slower fibrinolysis with strain. Our data suggest this is the case (Figure S9). Interestingly,  $v_r$  scales with  $K_D^{1/2}$ . Thus, strong binding (low  $K_D$ ) is predicted to actually hinder fibrinolysis, as the plasmin is unable to penetrate deeply into the clot, and is therefore limited to degrading only the surface.

Complementary derivations yield results similar to those presented here, showing that the key features of our model are not dependent on the choice of one particular theoretical framework. (supporting information, Figure S10). Equation 12 was compared to the experimental data and fit with a scaling factor of  $\sim 0.18$  to minimize the residuals between the data and the model (Figure 6a). This scaling factor likely arises from the uncertainties in applying literature values for  $k$  and  $K_D$  to our experimental system<sup>31</sup>.

## Discussion

### A simple model connects fibrinolysis rates to strain

Studies on biomaterials and tissues, including purified collagen<sup>27</sup>, fibrin<sup>16</sup>, bovine tail tendon<sup>28</sup>, annulus fibrosus<sup>29</sup>, and rabbit tendons<sup>30</sup> show that strain in general (though not always) slows the rate of proteolytic degradation at a macroscopic scale. However, single-molecule studies show that mechanical stretch speeds up proteolysis of both isolated collagen I trimers and von Willebrand factor<sup>19,32</sup>. This apparent discrepancy in the effect of strain at the microscopic and macroscopic level was, to our knowledge, unresolved.

We show that application of 177% strain reduces fibrinolysis by plasmin 10 fold. An analytical model that couples plasmin diffusion and fibrin proteolysis correctly predicts the relationship between fibrin degradation and applied strain. In this model, strain increases the density of the fibrin clot (Figure S12), and thus decreases the rate of plasmin transport within the clot (Figure 6b). The result is a thinner diffusive layer at the clot boundary, and hence slower proteolysis. Fibrin is subject to mechanical load *in vivo* due to platelet action, wound contraction<sup>33</sup> and mechanical stress at the wound site. Our data suggest that the properties of the fibrin network have evolved to protect mechanically loaded fibrin from degradation, as expected given its physiological function in wound healing.

A major pathway for the degradation of blood clots is the activation of fibrin-bound plasminogen by tPA that is already present in the blood stream, or that is administered



during the treatment of myocardial infarction or stroke<sup>34–36</sup>. We anticipate that the physical principles governing this mechanism of clot dissolution mirror our observations. Specifically, eqn. 12 remains valid so long as the localized rate of fibrinolysis is proportional to the local tPA concentration. Indeed, pre-cast clots containing bound plasminogen that are exposed to tPA dissolve from the outside in and exhibit a reactive boundary layer, analogous to what we observe in our study<sup>16,37</sup>.

Fibrin gels are widely used in wound healing applications<sup>6</sup>. One of the major challenges in using fibrin gels for this and other medical applications is their relatively rapid degradation by proteases<sup>6</sup>. Heat denaturation is one method used to protect the fibrin from protease action<sup>38,39</sup>. We observed that heat-denatured fibrin has a similar radial ingress rate as stretched ( $v_r = 0.0139 \pm 0.00023 \mu\text{m/s}$ , versus  $v_r = 0.0141 \pm 0.00013 \mu\text{m/s}$  for 110% strain) fibrin. This observation and the pronounced diffusional anisotropy that accompanies stain both suggest that mechanically stretched fibrin may have presently unexploited biomedical uses (see below).

## Conclusions

Anisotropic diffusion has been observed in biological tissues such as intervertebral disk (bovine and human), bovine annulus fibrosus and articular cartilage<sup>21–25,40–43</sup>. Numerous growth factors, for example insulin-like growth factor (IGF) I and II, vascular endothelial growth factor (VEGF) and epithelial growth factors (EGFR) both reversibly bind to the extracellular matrix<sup>44–47</sup> and form gradients that are critical during growth and development<sup>46</sup>, wound healing<sup>47</sup>, vasculogenesis<sup>48</sup>, and cancer metastasis<sup>49</sup>. We speculate that anisotropic transport, either diffusional or advective<sup>50</sup>, in strained tissues may play presently unrecognized roles in guiding embryonic development and tissue regeneration.

Controlling vascular growth, neurogenesis, and other complex tissue patterning processes remains a preeminent challenge in tissue engineering. Previous work shows that cell growth patterns can be directed using aligned substrates<sup>51,52</sup>, growth factor gradients<sup>53–55</sup>, and by tuning the proteolytic susceptibility of the surrounding matrix<sup>56</sup>. We observe that strain modulates each of these parameters (fibril alignment, diffusive transport, and proteolytic susceptibility) in fibrin clots. Fibrin is already a material of choice for medical implants and tissue engineering due to its strength, biodegradability, and ability to encapsulate and slowly release a wide variety of small molecules and growth factors<sup>57–61</sup>. We suggest that mechanical strain may offer a useful means of tuning cell growth, differentiation, and morphology in fibrin-based biomaterials.

## Supplementary Material

Refer to Web version on PubMed Central for supplementary material.

## Acknowledgments

The authors acknowledge Marc Levenston and Andrew Spakowitz for their valuable insights and discussions. Jack Chai for help with data analysis, Jian Fung for initial conception of experiment and Sarah Heilshorn for the loan of critical instrumentation. The research was funded by the Stanford Graduate Fellowship (ASA), the NIH New Innovator Award 1-DP2-OD007078-01 (ARD), and the Burroughs-Wellcome Career Award at the Scientific Interface (ARD).

## References

1. Clark RA. Ann N Y Acad Sci. 2001; 936:355. [PubMed: 11460492]
2. Cesarman-Maus G, Hajjar KA. Br J Haematol. 2005; 129:307. [PubMed: 15842654]

3. Kolev K, Machovich R. *Thromb Haemostasis*. 2003; 89:610. [PubMed: 12669114]
4. Esmon CT, Fukudome K, Mather T, Bode W, Regan LM, Stearns-Kurosawa DJ, Kurosawa S. *Haematologica*. 1999; 84:254. [PubMed: 10189392]
5. Weisel JW. *Science*. 2008; 320:456. [PubMed: 18436761]
6. Ahmed TA, Dare EV, Hincke M. *Tissue Eng Part B Rev*. 2008
7. Jockenhoevel S, Zund G, Hoerstrup SP, Chalabi K, Sachweh JS, Demircan L, Messmer BJ, Turina M. *Eur J Cardiothorac Surg*. 2001; 19:424. [PubMed: 11306307]
8. Cummings CL, Gawlitta D, Nerem RM, Stegemann JP. *Biomaterials*. 2004; 25:3699. [PubMed: 15020145]
9. Currie LJ, Sharpe JR, Martin R. *Plast Reconstr Surg*. 2001; 108:1713. [PubMed: 11711954]
10. Kopp J, Jeschke MG, Bach AD, Kneser U, Horch RE. *Cell Tissue Banking*. 2004; 5:89. [PubMed: 15241004]
11. Lam WA, Chaudhuri O, Crow A, Webster KD, Li TD, Kita A, Huang J, Fletcher DA. *Nat Mater*. 2011; 10:61. [PubMed: 21131961]
12. Whittaker P, Przyklenk K. *Blood Cells, Mol, Dis*. 2009; 42:51. [PubMed: 19054699]
13. Brown AE, Litvinov RI, Discher DE, Purohit PK, Weisel JW. *Science*. 2009; 325:741. [PubMed: 19661428]
14. Brown AE, Litvinov RI, Discher DE, Weisel JW. *Biophys J*. 2007; 92:L39. [PubMed: 17172299]
15. Purohit PK, Litvinov RI, Brown AE, Discher DE, Weisel JW. *Acta Biomater*. 2011; 7:2374. [PubMed: 21342665]
16. Varju I, Sotonyi P, Machovich R, Szabo L, Tenekedjiev K, Silva MM, Longstaff C, Kolev K. *J Thromb Haemostasis*. 2011; 9:979. [PubMed: 21251205]
17. Weisel JW. *J Thromb Haemostasis*. 2011; 9:977. [PubMed: 21392256]
18. Matsumoto T, Sasaki J, Alsberg E, Egusa H, Yatani H, Sohmura T. *PLoS One*. 2007; 2:e1211. [PubMed: 18030345]
19. Adhikari AS, Chai J, Dunn AR. *J Am Chem Soc*. 2011; 133:1686. [PubMed: 21247159]
20. Braeckmans K, Remaut K, Vandenbroucke RE, Lucas B, De Smedt SC, Demeester J. *Biophys J*. 2007; 92:2172. [PubMed: 17208970]
21. Jackson A, Yao H, Brown MD, Yong Gu W. *Spine (Philadelphia)*. 2006; 31:2783.
22. Chiu EJ, Newitt DC, Segal MR, Hu SS, Lotz JC, Majumdar S. *Spine (Philadelphia)*. 2001; 26:E437.
23. Travascio F, Gu WY. *Ann Biomed Eng*. 2011; 39:53. [PubMed: 20686922]
24. Leddy HA, Haider MA, Guilak F. *Biophys J*. 2006; 91:311. [PubMed: 16603503]
25. Travascio F, Jackson AR, Brown MD, Gu WY. *J Orthop Res*. 2009; 27:1625. [PubMed: 19489044]
26. Crank, J. *The mathematics of diffusion*. 2. Clarendon Press; Oxford, Eng: 1975.
27. Flynn BP, Bhole AP, Saeidi N, Liles M, Dimarzio CA, Ruberti JW. *PLoS One*. 2010; 5:e12337. [PubMed: 20808784]
28. Willett TL, Labow RS, Avery NC, Lee JM. *Ann Biomed Eng*. 2007; 35:1961. [PubMed: 17763961]
29. Lotz JC, Hadi T, Bratton C, Reiser KM, Hsieh AH. *Eur Spine J*. 2008; 17:1149. [PubMed: 18668268]
30. Nabeshima Y, Grood ES, Sakurai A, Herman JH. *J Orthop Res*. 1996; 14:123. [PubMed: 8618154]
31. Kastrikina TF, Taran LD, Kudinov SA. *Thromb Res*. 1986; 41:681. [PubMed: 2938303]
32. Zhang X, Halvorsen K, Zhang CZ, Wong WP, Springer TA. *Science*. 2009; 324:1330. [PubMed: 19498171]
33. Kilarski WW, Samolov B, Petersson L, Kvanta A, Gerwins P. *Nat Med*. 2009; 15:657. [PubMed: 19483693]
34. Tanne D, Gorman MJ, Bates VE, Kasner SE, Scott P, Verro P, Binder JR, Dayno JM, Schultz LR, Levine SR. *Stroke*. 2000; 31:370. [PubMed: 10657408]
35. Mateen FJ, Nasser M, Spencer BR, Freeman WD, Shuaib A, Demaerschalk BM, Wijedicks EF. *Mayo Clin Proc*. 2009; 84:334. [PubMed: 19339651]

36. Marler JR. N Engl J Med. 1995; 333:1581. [PubMed: 7477192]
37. Collet JP, Park D, Lesty C, Soria J, Soria C, Montalescot G, Weisel JW. Arterioscler Thromb Vasc Biol. 2000; 20:1354. [PubMed: 10807754]
38. Kassir I, Zangi L, Rivkin R, Levdansky L, Samuel S, Marx G, Gorodetsky R. Bone Marrow Transplant. 2006; 37:967. [PubMed: 16670702]
39. Rivkin R, Ben-Ari A, Kassir I, Zangi L, Gaberman E, Levdansky L, Marx G, Gorodetsky R. Cloning Stem Cells. 2007; 9:157. [PubMed: 17579550]
40. Hsu EW, Setton LA. Magn Reson Med. 1999; 41:992. [PubMed: 10332883]
41. Jackson AR, Yuan TY, Huang CY, Travascio F, Yong Gu W. Spine (Philadelphia). 2008; 33:1.
42. Ohshima H, Tsuji H, Hirano N, Ishihara H, Katoh Y, Yamada H. Spine (Philadelphia). 1989; 14:1234.
43. Travascio F, Zhao W, Gu WY. Ann Biomed Eng. 2009; 37:813. [PubMed: 19224367]
44. Bhakta NR, Garcia AM, Frank EH, Grodzinsky AJ, Morales TI. J Biol Chem. 2000; 275:5860. [PubMed: 10681577]
45. Garcia AM, Szasz N, Trippel SB, Morales TI, Grodzinsky AJ, Frank EH. Arch Biochem Biophys. 2003; 415:69. [PubMed: 12801514]
46. Thorne RG, Hrabetova S, Nicholson C. J Neurophysiol. 2004; 92:3471. [PubMed: 15269225]
47. Patil AS, Sable RB, Kothari RM. J Cell Physiol. 2011
48. Herbert SP, Stainier DY. Nat Rev Mol Cell Biol. 2011; 12:551. [PubMed: 21860391]
49. Sheng Q, Liu J. Br J Cancer. 2011; 104:1241. [PubMed: 21364581]
50. Rutkowski JM, Swartz MA. Trends Cell Biol. 2007; 17:44. [PubMed: 17141502]
51. Saez A, Ghibaud M, Buguin A, Silberzan P, Ladoux B. Proc Natl Acad Sci U S A. 2007; 104:8281. [PubMed: 17488828]
52. Dubey N, Letourneau PC, Tranquillo RT. Biomaterials. 2001; 22:1065. [PubMed: 11352087]
53. Rosoff WJ, McAllister R, Esrick MA, Goodhill GJ, Urbach JS. Biotechnol Bioeng. 2005; 91:754. [PubMed: 15981274]
54. Zisch AH, Ehrbar M, Djonov VG, Schnell C, Tschanz SA, Martiny-Baron G, Schenk U, Wood J, Burri PH, Hubbell JA. Circ Res. 2004; 94:1124. [PubMed: 15044320]
55. Shoichet M, Moore K, Macsween M. Tissue Eng. 2006; 12:267. [PubMed: 16548685]
56. Herbert CB, Bittner GD, Hubbell JA. J Comp Neurol. 1996; 365:380. [PubMed: 8822177]
57. Tsourvakas S, Alexandropoulos C, Karatzios C, Egnatiadis N, Kampagiannis N. Acta Orthop Belg. 2009; 75:537. [PubMed: 19774823]
58. Sakiyama-Elbert SE, Taylor SJ, McDonald JW. J Controlled Release. 2004; 98:281.
59. Sakiyama-Elbert SE, Willerth SM. Adv Drug Deliver Rev. 2007; 59:325.
60. Edelhauser HF, Cruysberg LPJ, Nuijts RMMA, Gilbert JA, Geroski DH, Hendrikse F. Curr Eye Res. 2005; 30:653. [PubMed: 16109645]
61. Tremblay P, Lord-Fontaine S, Yang F, Diep Q, Dergham P, Munzer S, McKerracher L. J Neurotraum. 2008; 25:1309.

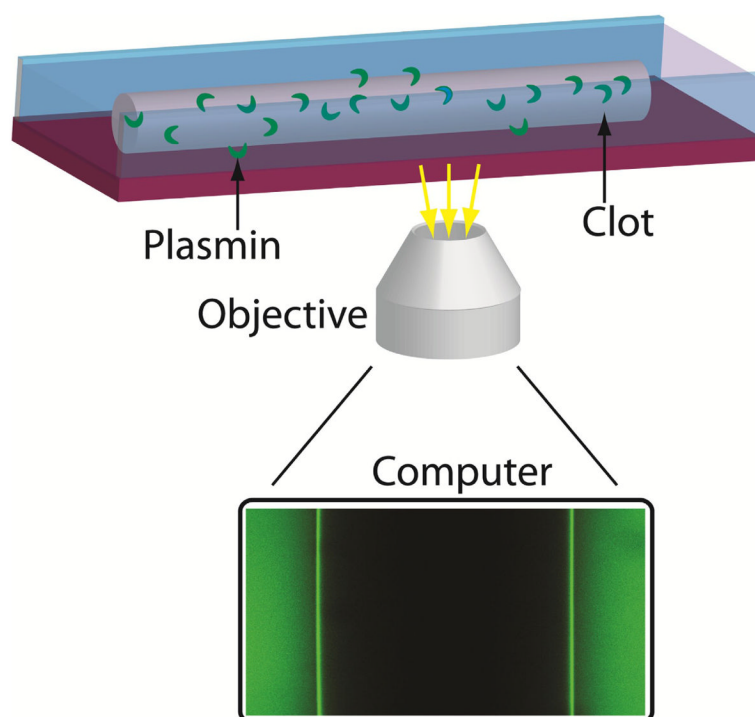


**Figure 1.** Experimental setup. The insert shows a confocal image of the fibrin clot with FITC-labeled plasminogen localized to the edges.

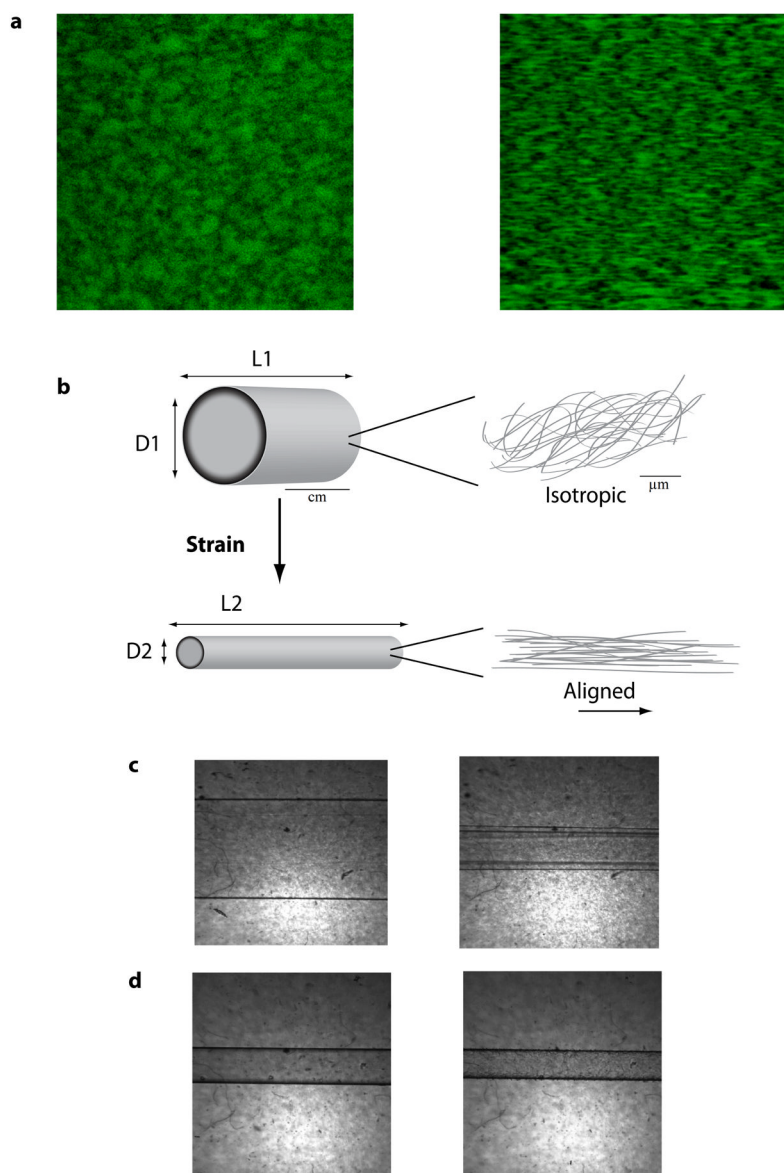


**Figure 2.**

**a)** Fibrin fibrils align under strain. Clots are formed in the presence of FITC-labeled dextran. The dark regions reflect dextran exclusion by the fibrin fibrils. Both the fibrils and voids are isotropic in unstrained clots (*left*), but align under 140% strain (*right*). **b)** Cartoon showing the decrease in clot radius and increase in fibril alignment upon application of strain. **c)** Images of an unstrained fibrin clot before and after 1000 seconds of plasmin-mediated degradation. **d)** Clot under 140% strain, before and after 1000 seconds of proteolysis. Note the smaller starting diameter, and the smaller decrease in radius relative to the unstrained clot.

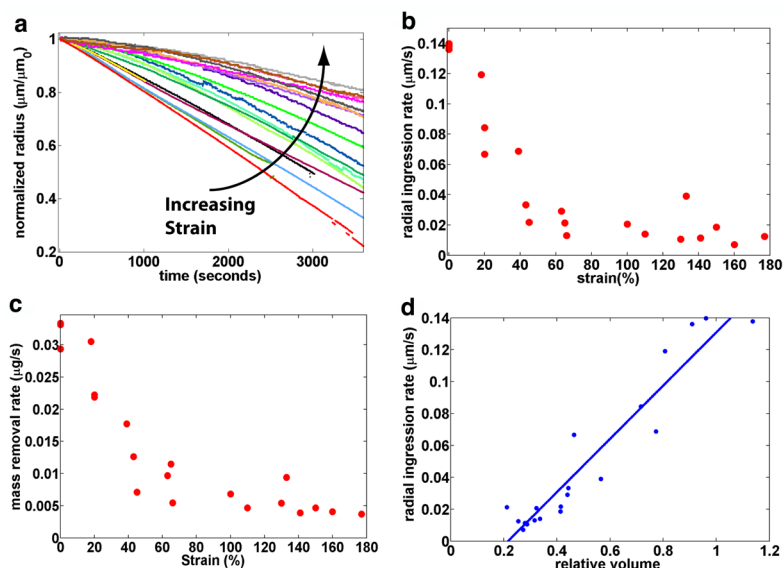


**Figure 3.**

Fibrinolysis as a function of applied strain. **a)** Normalized radius of the fibrin clots as a function of time. Proteolysis rates decrease as a function of strain, as indicated by the curved arrow. Unless otherwise specified, conditions used throughout are  $1.11 \text{ units mL}^{-1}$  plasmin,  $10 \text{ mM MES}$ ,  $100 \text{ mM NaCl}$ ,  $\text{pH } 7.4$ . **b)** Rate of clot radius decrease (radial ingress rate,  $v_r$ ) vs. strain. **c)** Rate of mass removal vs. strain. The change in radius is used to calculate the volume removed over time, which together with the known fibrin density (Supporting Information), yields the mass removal rate. **d)** The radial ingress rate scales linearly with the clot volume, and inversely with clot density. The error bars on the radial ingress rates are small compared to the size of the dots.

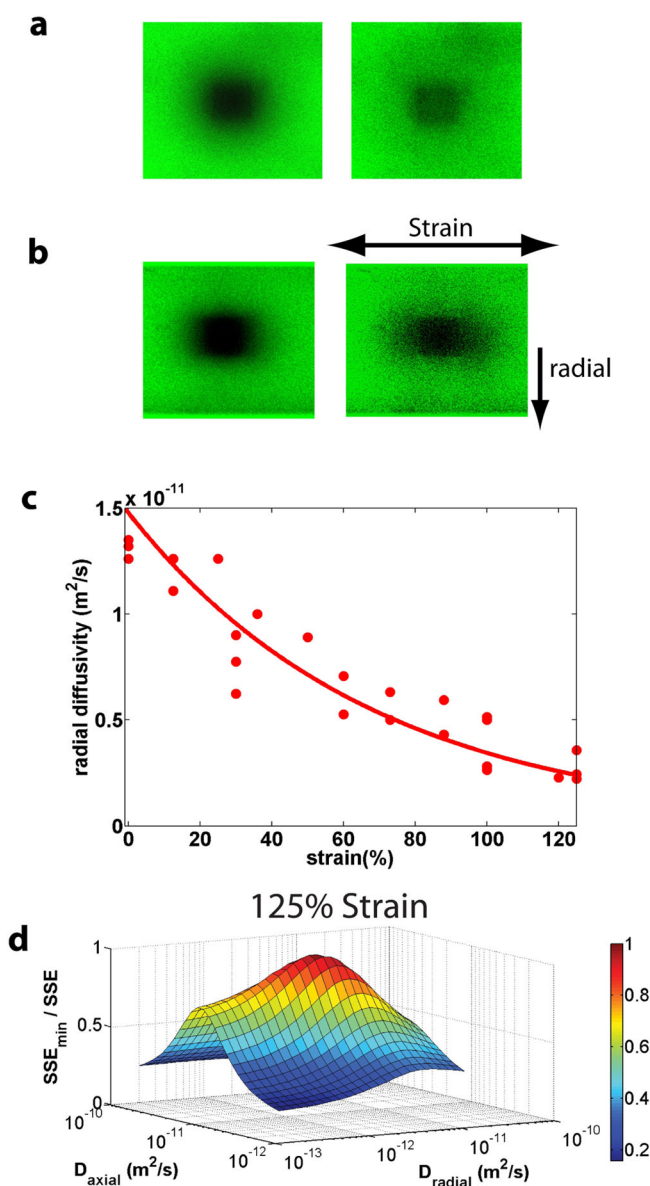


**Figure 4.**

Diffusivity is anisotropic in strained fibrin clots. **(a, b)** Confocal FRAP images of FITC-dextran within in fibrin clot at 0 seconds (*left*) and 200 seconds (*right*) after photobleaching. **a)** 0% strain; **b)** 100% strain. **c)** Radial diffusivity decreases 6-fold with 125% strain. Data are shown fit to a single exponential with a decay constant of  $0.0146 \pm 0.0012$ . **d)** A plot of minimum sum-squared-error ( $\text{SSE}_{\min}$ ) divided by SSE for range of axial and radial diffusion coefficients for FRAP data collected at 125% strain. Similar analyses for each FRAP measurement show that the fits values for axial and radial diffusivities are well constrained in all cases.



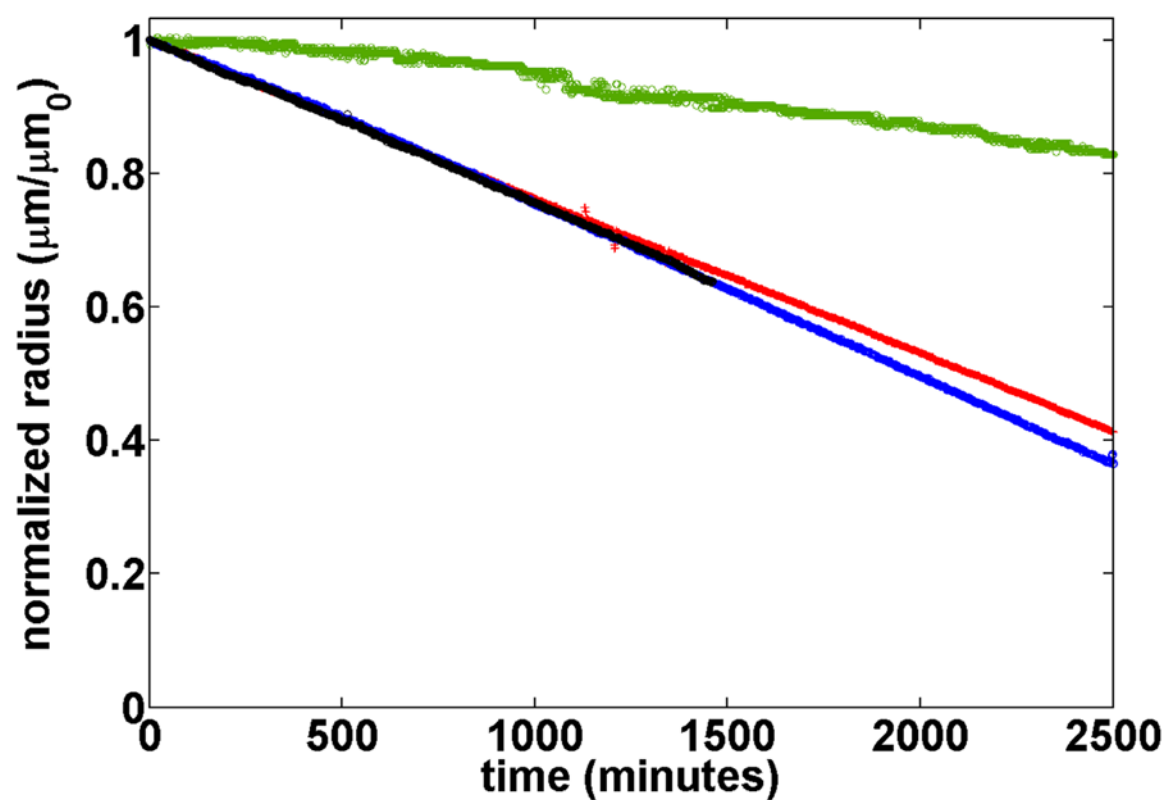


**Figure 5.**

Irreversible fibrin unfolding is not necessary to account for decreased proteolysis rates in strained fibrin clots. *Green*: 100% strain, *Red*: 0% strain. *Black*: 100% prestrained and relaxed, *Blue*: 125% prestrained and relaxed. The relaxed clots follow the same proteolysis profile as unstrained clots.

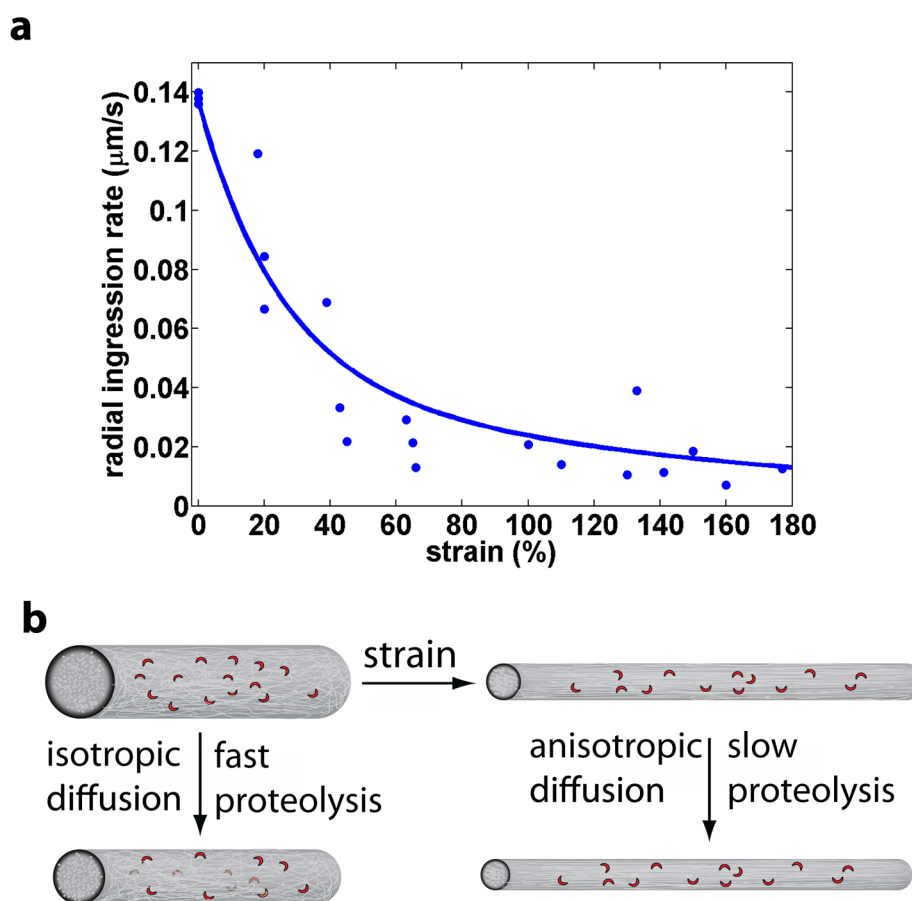


**Figure 6.**

**a)** Radial ingress rate vs. strain. Blue dots are the experimental data. The solid curve is the fit to eqn. 12. **b)** Schematic showing the effect of strain on diffusion and proteolysis. In the absence of strain, the fibrils in the clots are unaligned, the pore size is large, and the boundary layer in which proteolysis occurs is relatively wide. Under strain, the fibrils align and clot density increases. Transport is hindered and the proteolysis rate goes down.